International Journal of Solids and Structures 46 (2009) 4369–4378

Contents lists available at ScienceDirect

International Journal of Solids and Structures

journal homepage: www.elsevier.com/locate/ijsolstr

Over-nonlocal gradient enhanced plastic-damage model for concrete

Leong Hien Poh, Somsak Swaddiwudhipong *

Department of Civil Engineering, National University of Singapore, E1A-07-03, 1 Engineering Drive 2, Singapore 119260, Singapore

ARTICLE INFO

Article history:
Received 13 May 2009
Received in revised form 25 August 2009
Available online 2 September 2009

Keywords:
Plastic-damage models
Concrete
Localization
Nonlocal continuum
Gradient models

ABSTRACT

Classical continuum models exhibit strong mesh dependency during softening. One method to regularize the problem is to introduce a length scale parameter via the nonlocal formulation. However, standard nonlocal enhancement (either by integral or gradient formulation) may serve only as a partial localization limiter for many material models. The "over-nonlocal" formulation, where the weight for the nonlocal value is greater than unity and the excesses compensated by assigning a negative weight to the local value, is able to fully regularize certain material models when standard nonlocal enhancement fails to do so. A plastic-damage model for concrete is formulated with this over-nonlocal enhancement via the gradient approach and the full regularizing capabilities demonstrated.

1. Introduction

The accuracy of concrete models has improved tremendously over the years, and increasingly sophisticated models have been proposed to capture the material responses over a wide spectrum of load conditions. Anisotropic damage models provide good representations of microcrack evolutions since concrete responses are different under tension and compression respectively (e.g. Chaboche et al., 1995; Cicekli et al., 2007; Voyiadjis et al., 2008). However, the fourth order damage tensor, especially when coupled with plasticity, complicates the numerical implementation greatly. Isotropic damage assumption, although not as versatile under multiaxial stress states, usually produce reasonable results for most load conditions and is thus widely used due to its simplicity (e.g. Gatuingt and Pijaudier-Cabot, 2002; Grassl and Jirásek, 2006a; Nguyen and Korsunsky, 2008). An important aspect of concrete simulations is to study the material response until near failure state. However, the boundary value problem becomes ill-posed during softening and classical continuum models are unable to provide meaningful post-peak results. Numerically, these models exhibit strong pathological dependence on the orientation and size of the finite element mesh during softening (Bažant, 1976). To the limit of infinitesimal element size, the softening behavior localizes to a set of zero volume and the material response approaches that of perfectly brittle behavior. An extensive overview on the regularization techniques to obtain meaningful results is given by Bažant and Jirásek (2003).

One of the simplest remedy is the crack band model (Bažant and Oh, 1983), an ad hoc numerical treatment. Such models require the estimation of the crack band width and relating it to the element size in the localization zone. The stress–strain responses for these elements are scaled such that the energy dissipation is similar to the fracture energy, hence avoiding the spurious mesh dependency problem. This concept is employed in many plastic-damage models where a parameter controlling the slope of the softening curve is linked to the fracture energy and the smallest element size to provide partial regularization (e.g. Cicekli et al., 2007; Grassl and Jirásek, 2006a; Wu et al., 2006). Despite the relative ease of implementation, this approach is useful only if the localized zone can be deduced in advance. Moreover, it is difficult to extend such models for mixed mode failures, since the scaling is largely based on tensile fracture.

The softening behavior in concrete is largely due to the emergence, interactions and growth of microcracks. At this microscale range, the local strain field is inadequate to characterize the behavior of the microcracks. The softening phenomenon can be assumed to be dependent on the energy dissipation over a representative volume. This provides a physical basis for nonlocal formulation of concrete models. In a nonlocal continuum, the quantity at a point depends on the spatial average of the corresponding field over its neighborhood, and a material length scale is introduced through this radius of interaction. For concrete models, this length scale can be related to the maximum aggregate size (Bažant and Pijaudier-Cabot, 1989). Bažant et al. (1984) were among the pioneers to apply this concept as a localization limiter. However, numerical implementation of the nonlocal integral formulation typically requires a global averaging procedure and the resulting equations are difficult to express in the incremental form.

* Corresponding author. Tel.: +65 65162173; fax: +65 67791635.
E-mail address: cvesomsa@nus.edu.sg (S. Swaddiwudhipong).

0020-7683/$ - see front matter © 2009 Elsevier Ltd. All rights reserved.
doi:10.1016/j.ijsolstr.2009.08.025

Nevertheless, nonlocal integral formulation has been applied successfully on many plastic-damage models (e.g. Belnoue et al., 2007; Grassl and Jirásek, 2006b; Mohamad-Hussein and Shao, 2007; Nguyen and Korsunsky, 2008).

An alternative regularizing technique which is closely related to the integral approach is the gradient formulation. Peerlings et al. (1996) proposed the implicit gradient enhancement by satisfying an additional Helmholtz equation in a weak sense. This framework is numerically attractive since the governing equations can be discretized easily and which require only C^0 continuity. Moreover, the implicit gradient enhancement is strongly nonlocal and is similar to the integral formulation by assuming a particular Green's function and boundary conditions (Peerlings et al., 2001). Gradient enhanced damage models (e.g. Geers et al., 2000; Peerlings et al., 1998; Samal et al., 2008) and plastic-damage model (e.g. Addessi et al., 2002; de Borst et al., 1999) have demonstrated the ability to serve as localization limiters during softening.

Another class of gradient enhancements is the explicit gradient framework where the nonlocal terms are explicitly dependent on the gradient of some softening parameters. Such formulation typically results in higher order boundary conditions on the internal plastic/ damage domain which is not known a priori, leading to C^1 continuity requirements (de Borst and Pamin, 1996). Recently, Abu Al-Rub and Voyiadjis (2005) have developed a numerical scheme that requires only C^0 elements for the explicit gradient formulation, and have demonstrated its regularizing capabilities in a plastic-damage model for concrete (Abu Al-Rub and Voyiadjis, 2009).

Di Luzio and Bažant (2005) studied the localization behavior of several softening material models and reported that standard nonlocal enhancement (either by integral or gradient formulation) may not fully regularize the problem for certain material models. Vermeer and Brinkgreve (1994) had earlier proposed that the effective parameter be the weighted sum of the local and nonlocal values. For the integral approach, the problem is correctly regularized when the weight for the nonlocal parameter is set greater than unity, thus the term "over-nonlocal". This concept was adopted in the microplane model for concrete and full regularization was achieved where the standard integral formulation fails to do so (Di Luzio, 2007). Recently, Poh and Swaddiwudhipong (2009) have also reported that the over-nonlocal concept is applicable for the implicit gradient formulation using the linear softening von Mises model.

This paper adopts the plastic-damage model for concrete by Grassl and Jirásek (2006a) whom have shown its versatility over a wide spectrum of loading conditions in the original paper. Although the authors have noted that full regularization of this model is achieved only with the over-nonlocal formulation for the integral approach, it was not implemented in their subsequent refinement (Grassl and Jirásek, 2006b). This paper adopts the abovementioned plastic-damage model and demonstrates full regularization during softening with over-nonlocal enhancement via the gradient approach.

2. Theoretical framework for concrete model

The adopted concrete model is summarized in this section for completeness. Detailed explanations have been presented by Grassl and Jirásek (2006a).

The yield function f_p is defined in the principal effective stress space (Haigh-Westergaard coordinates) as:

$$f_p = \left\{ [1-q_h(\kappa_p)]\left(\frac{\bar{\rho}}{\sqrt{6}f_c}+\frac{\bar{\sigma}_v}{f_c}\right)^2 + \sqrt{\frac{3}{2}}\frac{\bar{\rho}}{f_c}\right\}^2 + m_0 q_h^2(\kappa_p)\left[\frac{\bar{\rho}}{\sqrt{6}f_c}r(\cos\bar{\theta})+\frac{\bar{\sigma}_v}{f_c}\right] - q_h^2(\kappa_p) \tag{1}$$

where

$\bar{\sigma}_v = \frac{I_1}{3}$, $I_1 = \bar{\boldsymbol{\sigma}} : \boldsymbol{\delta}$, $\bar{\boldsymbol{\sigma}}$ is the effective stress tensor;
$\bar{\rho} = \sqrt{2J_2}$, $J_2 = \frac{1}{2}\bar{\mathbf{S}} : \bar{\mathbf{S}}$, $\bar{\mathbf{S}}$ is the deviatoric effective stress tensor;
f_c is the uniaxial compressive strength;
q_h is a dimensionless function incorporating the hardening variable κ_p.

Lode angle $\bar{\theta} = \frac{1}{3}\arccos\left(\frac{3\sqrt{3}}{2}\frac{J_3}{J_2^{3/2}}\right)$, $J_3 = \frac{1}{3}\bar{\mathbf{S}}^3 : \boldsymbol{\delta}$

$$r(\cos\bar{\theta}) = \frac{4(1-e^2)\cos^2(\bar{\theta}) + (2e-1)^2}{2(1-e^2)\cos\bar{\theta} + (2e-1)\sqrt{4(1-e^2)\cos^2\bar{\theta} + 5e^2 - 4e}} \tag{2}$$

The function r controls the deviatoric section of the yield function, changing from triangular to circular shape when pressure increases. Eccentricity parameter e and friction parameter m_0 are material parameters calibrated from experimental data.

For realistic modeling of the volumetric expansion under compression in the plastic regime, non-associative flow rule is assumed. The plastic potential g_p is defined as:

$$g_p = \left\{ [1-q_h(\kappa_p)]\left(\frac{\bar{\rho}}{\sqrt{6}f_c}+\frac{\bar{\sigma}_v}{f_c}\right)^2 + \sqrt{\frac{3}{2}}\frac{\bar{\rho}}{f_c}\right\}^2 + q_h^2(\kappa_p)\left(\frac{m_0\bar{\rho}}{\sqrt{6}f_c}+\frac{m_g(\bar{\sigma}_v)}{f_c}\right)$$

$$m_g(\bar{\sigma}_v) = A_g B_g f_c \exp\left(\frac{\bar{\sigma}_v - f_t/3}{B_g f_c}\right) \tag{3}$$

where the function m_g determines the volumetric and deviatoric parts of the flow direction, f_t is the uniaxial tensile strength, A_g and B_g are material parameters. Plastic flow rate is thus given by:

$$\dot{\boldsymbol{\varepsilon}}_p = \dot{\lambda}\frac{\partial g_p}{\partial \bar{\boldsymbol{\sigma}}} = \dot{\lambda}\mathbf{m}_p \tag{4}$$

Plastic hardening is accounted for via the function q_h:

$$q_h(\kappa_p) = \begin{cases} q_{h0} + (1-q_{h0})\kappa_p(\kappa_p^2 - 3\kappa_p + 3) & \text{if } \kappa_p < 1 \\ 1 & \kappa_p \geqslant 1 \end{cases} \tag{5}$$

The evolution law for the hardening variable κ_p is defined as:

$$\dot{\kappa}_p = \dot{\lambda}k_p, \quad k_p = \frac{\|\mathbf{m}_p\|\cos^2\bar{\theta}}{x_h(\bar{\sigma}_v)} \tag{6}$$

$x_h(\bar{\sigma}_v)$ is a scaling function dependent on the volumetric effective stress such that the model response is more ductile under compression, its definition given as:

$$x_h = \begin{cases} A_h - (A_h - B_h)\exp(-R_h(\bar{\sigma}_v)/C_h) & \text{if } R_h(\bar{\sigma}_v) \geqslant 0 \\ E_h\exp(-R_h(\bar{\sigma}_v)/F_h) + D_h & R_h(\bar{\sigma}_v) < 0 \end{cases} \tag{7}$$

where A_h, B_h, C_h and D_h are calibrated from experimental data. E_h and F_h are parameters to ensure smooth transition at $R_h = 0$, defined as:

$$R_h(\bar{\sigma}_v) = -\frac{\bar{\sigma}_v}{f_c} - \frac{1}{3}$$
$$E_h = B_h - D_h$$
$$F_h = \frac{(B_h - D_h)C_h}{B_h - A_h} \tag{8}$$

The isotropic damage component is linked to the evolution of plastic strain, and the internal damage parameter incremental $\dot{\kappa}_d$ is given by:

$$\dot{\kappa}_d = \begin{cases} 0 & \text{if } \kappa_p < 1 \\ \dot{\varepsilon}_{pV}/x_s(\bar{\sigma}_v) & \text{if } \kappa_p \geqslant 1 \end{cases} \tag{9}$$

where $\dot{\varepsilon}_{pV} = \dot{\boldsymbol{\varepsilon}}_p : \boldsymbol{\delta}$.

x_s is a softening ductility measure defined as:

$$x_s(\bar{\sigma}_v) = \begin{cases} 1 + A_s R_s^2(\bar{\sigma}_v) & \text{if } R_s(\bar{\sigma}_v) < 1 \\ 1 - 3A_s + 4A_s\sqrt{R_s(\bar{\sigma}_v)} & \text{if } R_s(\bar{\sigma}_v) \geqslant 1 \end{cases} \tag{10}$$

where A_s is a model parameter.

The dimensionless variable R_s is the ratio between the negative volumetric plastic strain rate $\dot{\varepsilon}^-_{pV}$ and the total volumetric plastic strain rate $\dot{\varepsilon}_{pV}$:

$$R_s = \dot{\varepsilon}^-_{pV}/\dot{\varepsilon}_{pV}$$

$$\dot{\varepsilon}^-_{pV} = \sum_{I=1}^{3}\langle -\dot{\varepsilon}_{pI}\rangle \tag{11}$$

where $\langle\cdot\rangle$ denotes the McAuley brackets.

The damage parameter ω is obtained from the internal damage parameter κ_d as:

$$\omega = 1 - \exp(-\kappa_d/\varepsilon_f) \tag{12}$$

where ε_f is a parameter which controls the slope of the softening curve.

Finally, the nominal stress is obtained as:

$$\boldsymbol{\sigma} = (1-\omega)\bar{\boldsymbol{\sigma}} \tag{13}$$

The concrete model is implemented in the finite element package (ABAQUS, 2003) via the UMAT subroutine. There are many material parameters for the constitutive model. Calibration can be minimized by assuming some of the parameters in the absence of experimental data (see Grassl and Jirásek, 2006a). Our model assumes the following parameters: $A_s = 15, D_f = 0.85, A_h = 0.02$, $B_h = 0.00075, C_h = 2$ and $D_h = 2.5 \times 10^{-7}$. These values are calibrated with existing experimental data, and are used for all simulations reported in this paper. The numerical implementations in this paper are in 3D. We reproduce two numerical results (Figs. 1 and 2) to illustrate the versatility of the model.

3. Mesh sensitivity

The plastic-damage concrete model exhibits strong mesh sensitivities during softening. For consistent load–displacement curves, the softening parameter ε_f has to be recalibrated for each mesh refinement. This is clearly not practical when predictions of material responses in the absence of experimental data are required. Moreover, local models also exhibit strong dependency on the

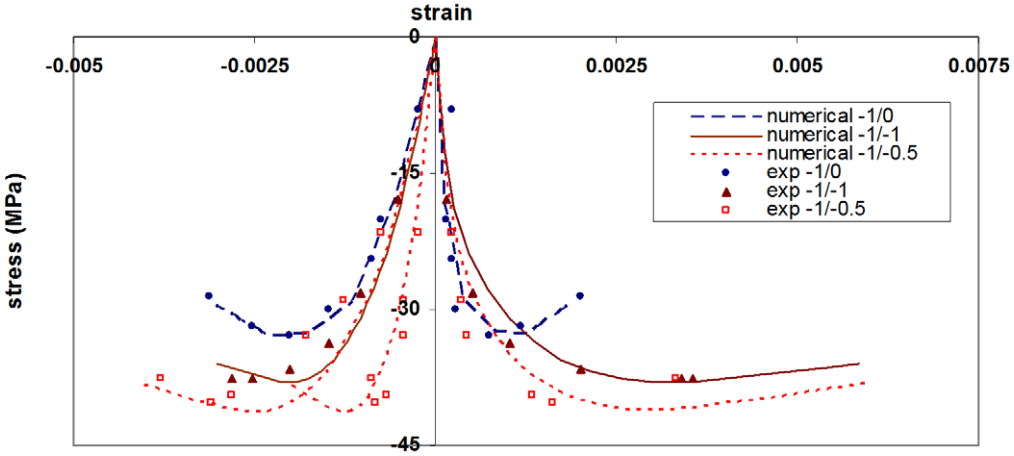

Fig. 1. Biaxial compression as reported by Kupfer et al. (1969). The material parameters are $E = 32$ GPa, $v = 0.18$, $f_c = 32.8$ MPa, $f_t = 3.3$ MPa and $\varepsilon_f = 165 \times 10^{-6}$.

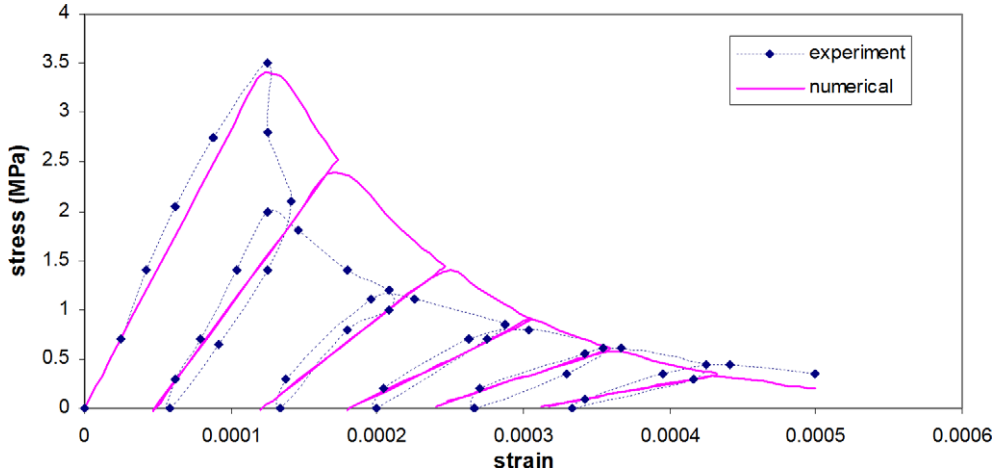

Fig. 2. Cyclical uniaxial tensile loading as reported by Gopalaratnam and Shah (1985). The material parameters are $E = 28$ GPa, $v = 0.2$, $f_c = 40$ MPa, $f_t = 3.5$ MPa and $\varepsilon_f = 130 \times 10^{-6}$.

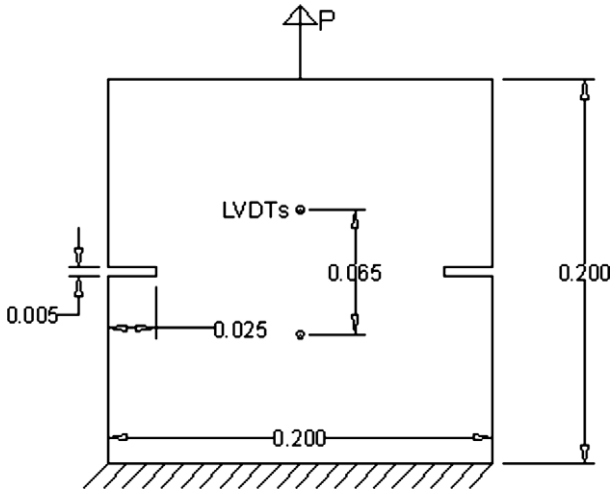

Fig. 3. DEN specimen geometry (m) in uniaxial tension.

mesh orientations. These problems will be illustrated in this section.

Material parameters ($E = 25\,\text{GPa}, \nu = 0.2, f_c = 44\,\text{MPa}, f_t = 2.5\,\text{MPa}, \varepsilon_f = 4.3 \times 10^{-3}$) are calibrated for a particular mesh (206 elements) according to the Double Edge Notched (DEN) uniaxial test by Van Mier and Nooru-Mohamed (1990), as depicted in Fig. 3. Only one quarter of the specimen has to be modeled due to the vertical and out-of-plane symmetry. When the same material parameters are used for different element mesh, numerical results are not meaningful as shown in Fig. 4. The contour diagrams in Fig. 5 depicting the damaged regions further demonstrates the pathological mesh dependencies of the concrete model, i.e., the damage region localizes to the smallest element size as well as propagate according to the mesh direction. The deformation contours are also of similar profiles. Due to strong localization induced by the notch, numerical results are not able to even predict a consistent peak force. The strong mesh dependency thus limits the usefulness of such local softening models.

4. Regularization by nonlocal damage

Softening behavior of the adopted concrete model is governed by the internal damage parameter κ_d. An intuitive approach is to regularize the problem by introducing nonlocality via this internal parameter. In the integral formulation, the nonlocal parameter is given by:

$$\bar{\kappa}_d(\mathbf{x}) = \frac{1}{\mathrm{V}(\mathbf{x})} \int_{\mathrm{v}} \alpha(\mathbf{y}, \mathbf{x}) \kappa_d(\mathbf{y}) d\nu \tag{14}$$

where $\mathbf{x}$, $\mathbf{y}$ are the coordinates vectors, $\alpha(\mathbf{y}, \mathbf{x})$ is the weight function and $\mathrm{V}(\mathbf{x}) = \int_{\mathrm{v}} \alpha(\mathbf{y}, \mathbf{x}) d\nu$ is the normalizing factor.

There is a subclass of nonlocal formulation where the effective parameter is the weighted sum of the nonlocal and local values respectively, first proposed by Vermeer and Brinkgreve (1994) and later implemented by Stromberg and Ristinmaa (1996). This

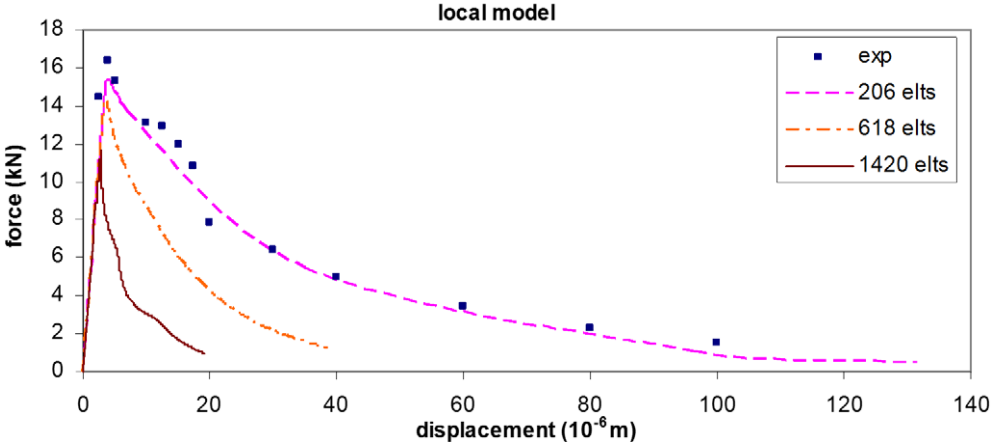

Fig. 4. Load displacement graphs for different mesh sizes.

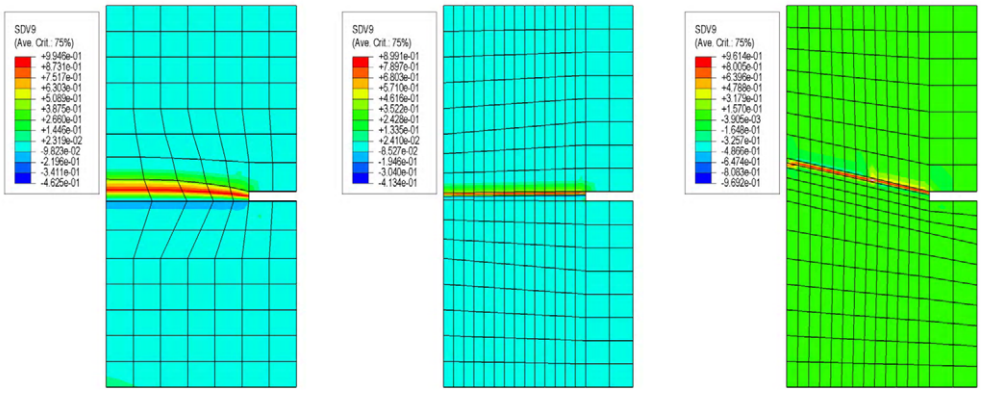

Fig. 5. Damage profiles for different mesh size and direction.

novel approach sets the weight for the nonlocal parameter, m, as greater than unity, compensating for the excesses by assigning a negative weight to the local component:

$$\hat{\kappa}_d(\mathbf{x}) = m\bar{\kappa}_d(\mathbf{x}) + (1-m)\kappa_d(\mathbf{x}) \tag{15}$$

For certain material models, full regularization during softening can be achieved only if parameter m is greater than unity, hence the term "over-nonlocal" (Di Luzio and Bažant, 2005; Jirásek and Grassl, 2004). This was numerically demonstrated by the over-nonlocal microplane model via the integral approach (Di Luzio, 2007). Poh and Swaddiwudhipong (2009) have recently reported the applicability of the over-nonlocal enhancement with the gradient formulation for the linear softening von Mises model. The gradient framework will be implemented for the adopted concrete model.

For the gradient approach, instead of Eq. (14), the nonlocal internal damage parameter $\bar{\kappa}_d$ is given by:

$$\bar{\kappa}_d(\mathbf{x}) - c\nabla^2\bar{\kappa}_d(\mathbf{x}) = \kappa_d(\mathbf{x}) \tag{16}$$

where c is the length scale parameter with units of length square. This nonlocal parameter $\bar{\kappa}_d$ then enters over-nonlocal expression in Eq. (15).

We can better understand the regularizing effects by carrying out a 1D spectral analysis of the constitutive model. The nominal stress rate $\dot{\boldsymbol{\sigma}}$ for the gradient enhanced model is given by:

$$\begin{aligned}\dot{\sigma} &= (1-\omega)\dot{\bar{\sigma}} - \dot{\omega}\bar{\sigma}\\ \omega &= 1 - \exp(-\hat{\kappa}_d/\varepsilon_f)\end{aligned} \tag{17}$$

where $\dot{\bar{\boldsymbol{\sigma}}}$ is the effective stress rate. Nonlocality is introduced into the damage function ω via the effective internal parameter $\hat{\kappa}_d$.

For the adopted concrete model, softening is activated only when maximum hardening is attained ($q_h = 1$). The yield function in Eq. (1) characterized by uniaxial tensile stress $\bar{\sigma}$ is given by:

$$f_p = \left(\frac{\bar{\sigma}}{f_c}\right)^2 + m_0(r+1)\bar{\sigma} - 1 = 0 \tag{18}$$

From the consistency equation, we have:

$$\dot{f}_p = 0 \Rightarrow \dot{\bar{\sigma}} = 0 \tag{19}$$

From Eqs. (18) and (19), we note that the effective stress $\bar{\sigma}$ is constant during uniaxial softening.

We substitute Eqs. (17a) and (19) into the equilibrium equation to obtain:

$$\dot{\sigma}_{,x} = 0 \Rightarrow \dot{\hat{\kappa}}_{d,x} = 0 \tag{20}$$

where $(\,)_{,x}$ implies differentiation of $(\,)$ with respect to x.

From Eq. (20), we can express $\dot{\hat{\kappa}}_d$ in terms of $\dot{\kappa}_d$:

$$\begin{aligned}\dot{\hat{\kappa}}_{d,x} &= m\dot{\bar{\kappa}}_{d,x} + (1-m)\dot{\kappa}_{d,x} = 0\\ \dot{\bar{\kappa}}_d &= \dot{\kappa}_d + \left(\frac{m-1}{m}\right)c\dot{\kappa}_{d,xx}\end{aligned} \tag{21}$$

We then obtain Eq. (20) as:

$$\dot{\hat{\kappa}}_{d,x} = \dot{\kappa}_{d,x} + c(m-1)\dot{\kappa}_{d,xxx} = 0 \tag{22}$$

A solution to Eq. (22) is the harmonic solution $\dot{\kappa}_d = Ae^{iKx}$ where A is the amplitude and K is the wave number. This is substituted into Eq. (22) to obtain:

$$K[1 + c(1-m)K^2] = 0 \tag{23}$$

For both the classical model ($c = 0\text{m}^2$) and the standard gradient enhancement ($m = 1$), the solution is not meaningful. A non-trivial solution $K_{cr} = \frac{1}{\sqrt{c(m-1)}}$ is obtained only when $m > 1$. For an arbitrary κ_d wave, larger wavelengths are dissipated by material damping and a stationary wavelength $\alpha_{cr} = 2\pi\sqrt{c(m-1)}$ is obtained. We note that the elastic yield surface for uniaxial compression during softening is given by $f_p = \left(\frac{\sigma}{f_c}\right)^2 - 1$. Using similar arguments from Eqs. (19)–(23), we arrive at similar conclusion that $m > 1$. This suggests that for the gradient enhancement, the over-nonlocal formulation is required to fully regularize the 1D problem.

It is interesting to note that in the spectral analysis where $m > 1$, Eq. (22) is of the explicit gradient expression which has been applied by other researchers to regularize softening behaviors (e.g. Abu Al-Rub and Voyiadjis, 2009). Using the linear softening von Mises model, (Poh and Swaddiwudhipong, 2009) have shown that different combinations of parameters m and c leading to the same α_{cr} value do not produce similar load displacement curves, despite having similar shear bandwidths. This can be considered as a drawback of the over-nonlocal model since it introduces an additional parameter m for calibration. Nevertheless, it was also reported that an m value of just over unity is able to fully regularize the problem whereas the standard formulation ($m = 1$) fails to do so. In the absence of experimental observations (e.g. width of micro-cracked region), it is suggested to adopt the value of m just slightly over unity to induce full regularization without affecting the load–displacement response. The length scale parameter c can then be calibrated from the load–displacement curves. Moreover, to correctly reproduce the strain fields in the over-nonlocal microplane model, Di Luzio (2007) has also recommended that $1 < m \leqslant 1.1$. This paper thus adopts a value of m which is just slightly greater than unity for the over-nonlocal gradient enhancement and the regularizing effects demonstrated in later sections.

5. Numerical framework

The over-nonlocal gradient enhanced concrete model is implemented in ABAQUS (2003) via the UEL subroutine. A brief discussion of the stiffness matrix is presented here. Ignoring body forces, the set of governing equations for finite element formulation comprises of the equilibrium equation and the implicit gradient Helmholtz equation respectively:

$$\begin{aligned}&\nabla\cdot\boldsymbol{\sigma} = 0\\ &\bar{\kappa}_d - c\nabla^2\bar{\kappa}_d = \kappa_d\end{aligned} \tag{24}$$

Both governing equations are satisfied in a weak sense with suitable weight functions $\mathbf{w}_1$ and w_2 to obtain:

$$\begin{aligned}&\int_v (\nabla\mathbf{w}_1)^T\boldsymbol{\sigma}dv = \int_s (\mathbf{w}_1)^T\mathbf{t}ds\\ &\int_v [(w_2)^T\bar{\kappa}_d + c(\nabla w_2)^T\nabla\bar{\kappa}_d]dv = \int_v (w_2)^T\kappa_d dv\end{aligned} \tag{25}$$

where superscript T implies transpose, $\mathbf{t} = \boldsymbol{\sigma}\cdot\mathbf{n}$ is the traction on the domain boundary (with a unit normal vector $\mathbf{n}$). The natural non-standard boundary condition $\nabla\bar{\kappa}_d\cdot\mathbf{n} = 0$ is typically adopted in literature (e.g. Peerlings et al., 1998, 2001) and will be assumed in this paper. If a thermodynamic force conjugate to the gradient term is defined, this boundary condition can be interpreted as a zero energy flux due to damage mechanisms across the boundary of the damaged zone (e.g. Forest, 2009).

This is then expressed in the incremental form to set up the framework for finite element implementation:

$$\int_v \left[(\nabla \mathbf{w}_1)^T d\boldsymbol{\sigma}\right] dv = \int_s (\mathbf{w}_1)^T \mathbf{t} ds - \int_v (\nabla \mathbf{w}_1)^T \boldsymbol{\sigma} dv - \int_v \left[(w_2)^T d\kappa_d\right] dv + \int_v \left[(w_2)^T d\bar{\kappa}_d + c(\nabla w_2)^T \nabla (d\bar{\kappa}_d)\right] dv = \int_v (w_2)^T \kappa_d dv - \int_v \left[(w_2)^T \bar{\kappa}_d + c(\nabla w_2)^T \nabla \bar{\kappa}_d\right] dv \quad (26)$$

The nodal degrees of freedom are discretized as:

$$u = \mathbf{N}^T \mathbf{a}, \quad \bar{\kappa}_d = \mathbf{N}^T \bar{\boldsymbol{\kappa}}_d \quad (27)$$

so that

$$\boldsymbol{\varepsilon} = \mathbf{B}\mathbf{a}, \quad \nabla \bar{\kappa}_d = \nabla \mathbf{N}^T \bar{\boldsymbol{\kappa}}_d \quad (28)$$

where **N**, **B** and **a** are the interpolation function matrix, the strain matrix and the nodal parameter vector respectively. The weight functions $\mathbf{w}_1$ and w_2 are assigned as **u** and $\bar{\kappa}$ respectively. We express $d\boldsymbol{\sigma}$ and $d\kappa_d$ in Eq. (26) in terms of the nodal degrees of freedom (see Appendix A) and the tangent stiffness matrix for an element is obtained:

$$\begin{bmatrix} \mathbf{K}_{11} & \mathbf{K}_{12} \\ \mathbf{K}_{21} & \mathbf{K}_{22} \end{bmatrix} \begin{bmatrix} d\mathbf{a} \\ d\bar{\boldsymbol{\kappa}}_d \end{bmatrix} = \begin{bmatrix} \mathbf{f}_1 \\ \mathbf{f}_2 \end{bmatrix} \quad (29)$$

where for a 20-node solid element, the sub-matrices are defined as:

$$\mathbf{f}_1 = \int_s \mathbf{N} \mathbf{t} ds - \int_v \mathbf{B}^T \boldsymbol{\sigma} dv$$

$$\mathbf{f}_2 = \int_v \kappa_d \mathbf{N} - [\bar{\kappa}_d \mathbf{N} + c(\nabla \mathbf{N})(\nabla \bar{\kappa}_d)] dv$$

$$\mathbf{K}_{11} = \int_v \{[\mathbf{B}^T]_{60\times 6} [\mathbf{a}_{11}]_{6x6} [\mathbf{B}]_{6\times 60}\} dv$$

$$\mathbf{K}_{12} = -\int_v \{[\mathbf{B}^T]_{60\times 6} [\mathbf{a}_{12}]_{6\times 1} [\mathbf{N}^T]_{1\times 20}\} dv$$

$$\mathbf{K}_{21} = -\int_v \{[\mathbf{N}]_{20\times 1} [\mathbf{a}_{21}]_{1\times 6} [\mathbf{B}]_{6\times 60}\} dv$$

$$\mathbf{K}_{22} = \int_v \{[\mathbf{N}]_{20\times 1} [\mathbf{N}^T]_{1\times 20} + c[\nabla \mathbf{N}]_{20\times 3} [\nabla \mathbf{N}^T]_{3\times 20}\} dv$$

with

$\mathbf{a}_{11}$ as the Voigt matrix for tensor $(1-\omega)\mathbf{D}_{ep}^{al} - \exp\left(\frac{-\bar{\kappa}_d}{\varepsilon_f}\right)\left(\frac{1}{\varepsilon_f}\right)(1-m)\bar{\boldsymbol{\sigma}} \otimes \mathbf{N}_a$;
$\mathbf{a}_{12}$ as the Voigt vector for tensor $\exp\left(\frac{-\bar{\kappa}_d}{\varepsilon_f}\right)\left(\frac{m}{\varepsilon_f}\right)\bar{\boldsymbol{\sigma}}$;
$\mathbf{a}_{21}$ as the Voigt vector for tensor $\mathbf{N}_a$;
ε_f, $\mathbf{D}_{ep}^{al}$ and $\mathbf{N}_a$ as defined in Eqs. (12), (A6) and (A8), respectively.

It is noted that the standard implicit gradient enhancement is recovered when parameter $m = 1$.

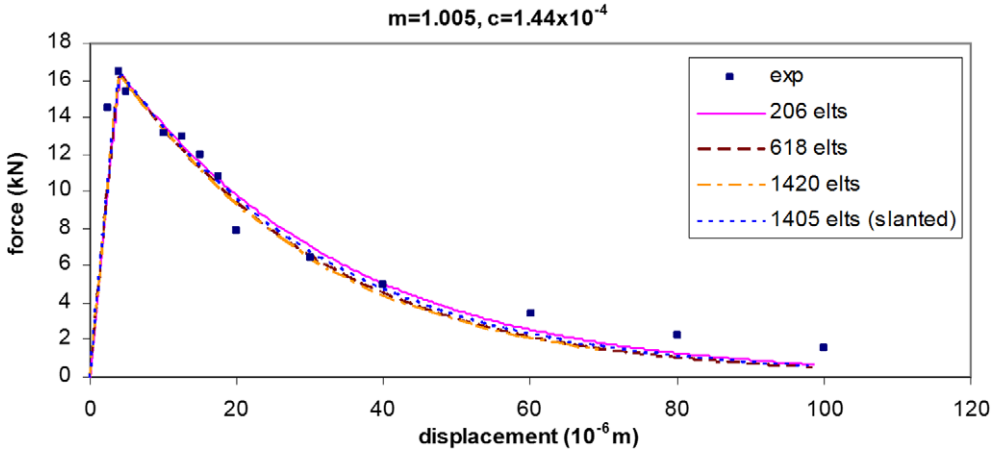

Fig. 6. Load displacement graphs for different element sizes.

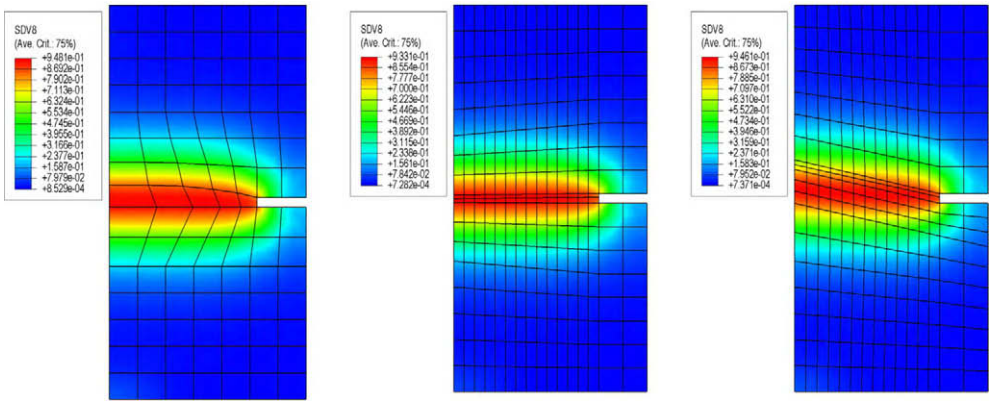

Fig. 7. Damage profiles for different mesh sizes and orientations.

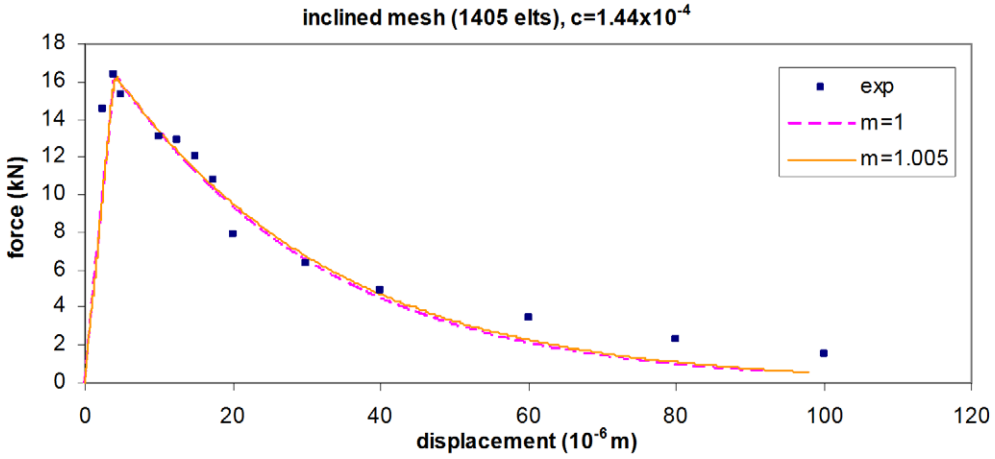

Fig. 8. Load displacement curves for $m = 1$ and $m = 1.005$.

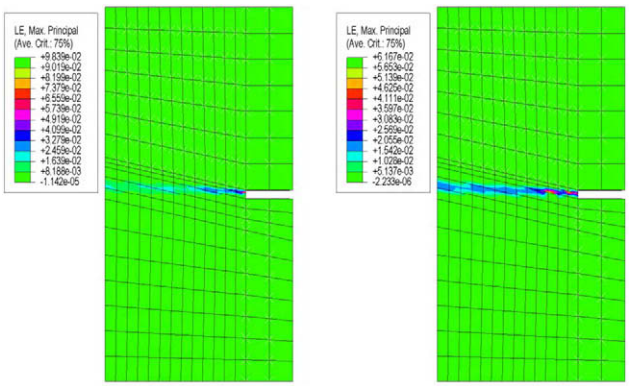

Fig. 9. Contour plots (maximum principal strain) for (a) $m = 1$ and (b) $m = 1.005$, respectively.

6. Numerical results

6.1. DEN specimen in uniaxial tension test

Numerical simulation for the DEN experiment in Section 3 is reanalyzed using the over-nonlocal gradient framework. The material parameters adopted are $E = 25$ GPa, $\nu = 0.2$, $f_c = 44$ MPa, $f_t = 2.5$ MPa, $\varepsilon_f = 9.5 \times 10^{-4}$, $m = 1.005$ and $c = 1.4 \times 10^{-4}$ m^2. The load–displacement graphs and the damage profiles are depicted in Figs. 6 and 7 respectively. By adopting the over-nonlocal enhancement, the numerical results are now objective, i.e., global responses converged upon mesh refinements and the damage profiles are consistent for different element sizes and orientations.

We then compare the numerical responses between the over-nonlocal ($m = 1.005$) and the standard nonlocal ($m = 1$) enhancements. The load–displacement graphs for the mesh with inclined orientation are depicted in Fig. 8. It is noted that the load displacement curves for the two m values are almost identical. The standard implicit gradient enhancement is able to produce converged global results upon mesh refinements. However, from the 1D spectral analysis, we expect the problem to be fully regularized only when $m > 1$. This can be seen from the contour plots in Fig. 9. The maximum principal strain is an indicator of the cracked path. For the standard implicit gradient model ($m = 1$), deformation tends to localize into the smallest element. With the over-nonlocal enhancement ($m = 1.005$), the crack propagates across the specimen width at failure, which is physically more acceptable. This example shows that for certain models, although the global response converges upon mesh refinements with standard nonlocal enhancements ($m = 1$), localization still occurs with discontinuous strain rates and the problem is only partially regularized (Jirásek and Grassl, 2004). The gradient approach of the over-nonlocal enhancement is able to fully regularize the localization problem. It is also noted that a slight increment from unity in the value of m parameter is able to induce full regularization during softening.

6.2. Four point bending of SEN beam

The next example is the more complicated four point bending experiment of a Single Edge Notched (SEN) beam conducted by

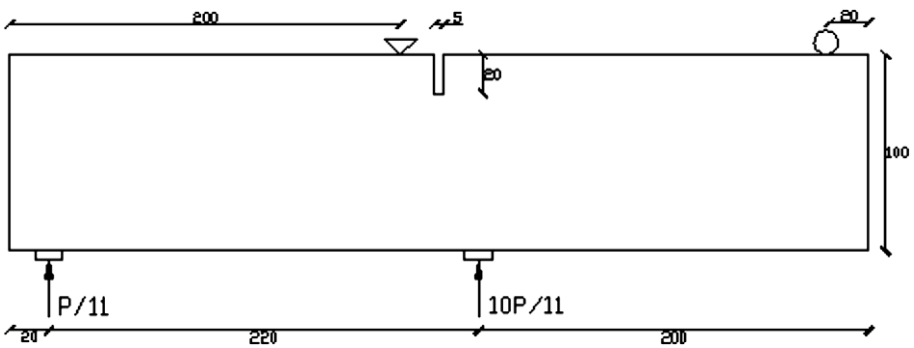

Fig. 10. SEN specimen geometry (mm) in four point bending.

Schlangen (1993), as depicted in Fig. 10. The anti-symmetric loading leads to a mixed mode I and II stress field at crack initiation which gradually degenerates to mode I failure. This results in a curved crack path initiating from the notch tip. Jirásek and Grassl (2008) have modeled a similar problem with different damage models and the simulated failure patterns are observed to be mesh sensitive.

The experiment is simulated with the over-nonlocal plastic-damage model discussed in Section 5. The material parameters adopted are $E = 30\,\text{GPa}, \nu = 0.2, f_c = 46\,\text{MPa}, f_t = 3\,\text{MPa}, \varepsilon_f = 9 \times 10^{-4}$ and $c = 1.4 \times 10^{-4}\,\text{m}^2$. As in the previous section, parameter m is assumed to be 1.005. The steel loading platens are set stiffer than the concrete beam reflecting the effect of their modulus ratio and a point load is applied at the centre of the platens. For such a com-

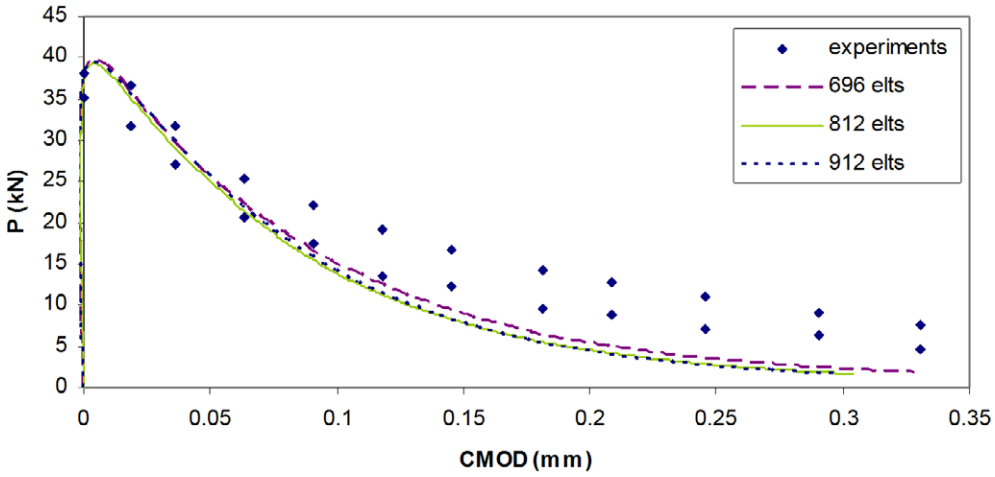

Fig. 11. Load – CMOD graph.

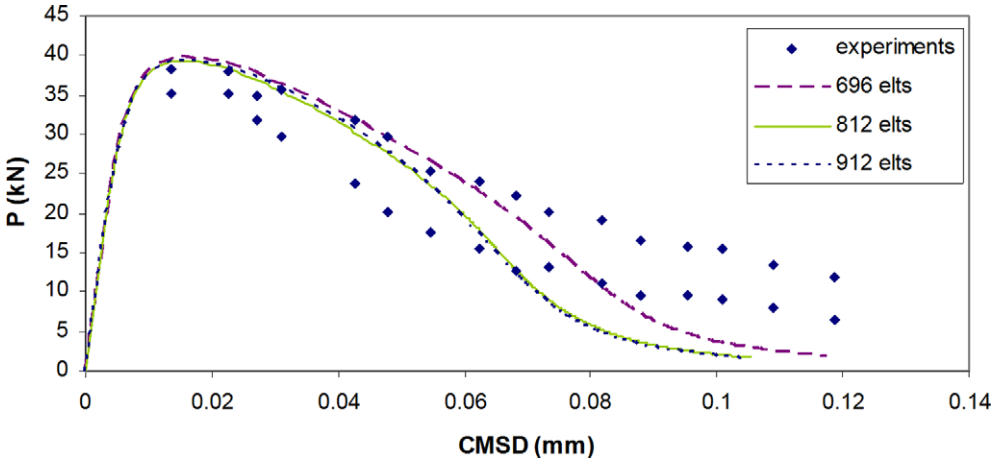

Fig. 12. Load – CMSD graph.

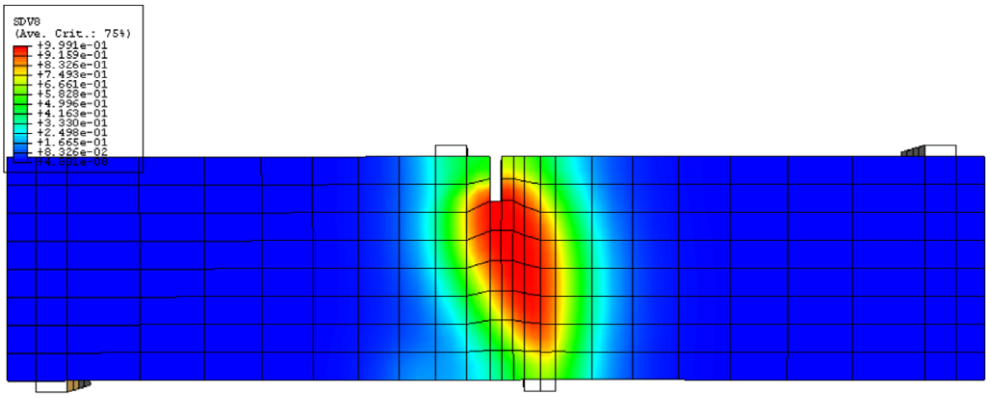

Fig. 13. Damage profile.

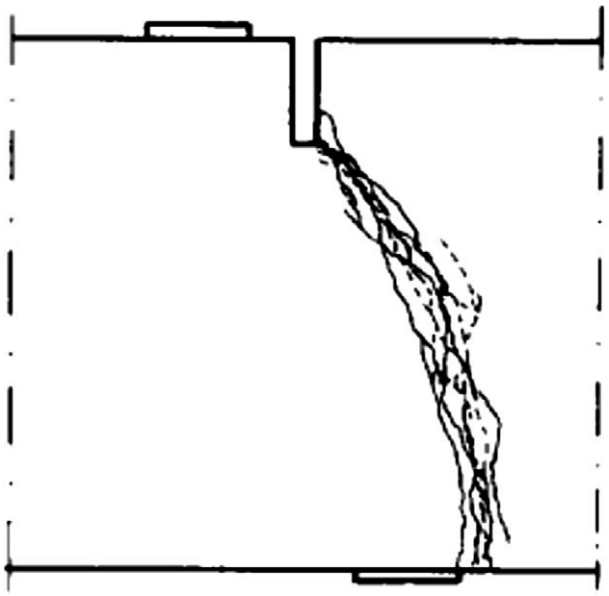

Fig. 14. Experimental crack patterns..(Schlangen, 1993).

plicated loading, it is not sufficient to consider only one load–displacement diagram. Thus, the load is plotted against the crack mouth opening displacement (CMOD) and sliding displacement (CMSD) in Figs. 11 and 12 respectively. Mesh refinements are adopted near the notch where the crack is propagating. It is shown that the over-nonlocal model is able to reproduce satisfactory results, although the numerical responses are too brittle in the later stages of the softening regime. This may be improved by adopting a more complicated anisotropic damage evolution. The damage profile is illustrated in Fig. 13, capturing the curved crack pattern observed experimentally (Fig. 14). As parameter m is set at 1.005, the damaged band can be calibrated by the length scale parameter c if necessary. As depicted, the damaged zone is able to traverse across elements of different sizes, demonstrating the mesh objectivity of the over-nonlocal gradient enhanced model for the more complicated loading conditions.

7. Conclusion

The adopted plastic-damage model has been reported to give good numerical results over a large range of load conditions. However, the local constitutive model suffers from strong mesh dependencies during softening. The standard nonlocal enhancements, either by integral or gradient approach, have been reported to regularize many softening models. However, for certain material models, they fail as full localization limiter. One remedy is to adopt the over-nonlocal enhancement, which has been reported to be a viable alternative for several models. Just a slight increment from unity for the parameter m is able to induce full regularization during softening. Several examples in literature adopt the integral approach in the over-nonlocal formulation. This paper illustrates the regularizing capabilities of the over-nonlocal formulation via the gradient approach for a more sophisticated plastic-damage model for concrete. It is noted that the global force–displacement numerical results are almost identical between the standard gradient enhancement and the over-nonlocal formulation when m is close to unity. However, in situations where very fine meshes are required (for example, a small notch size) or when the orientations of the elements are irregular due to geometry constraints, the over-nonlocal method is advantageous since it is truly mesh independent, as compared to the standard gradient enhancement whereby deformation is still mesh sensitive for certain models.

Appendix A

At each time step, the stress increment is given by:

$$d\boldsymbol{\sigma} = (1-\omega)d\bar{\boldsymbol{\sigma}} - d\omega\bar{\boldsymbol{\sigma}} = (1-\omega)d\bar{\boldsymbol{\sigma}} - \exp\left(\frac{-\hat{\kappa}_d}{\varepsilon_f}\right)\left(\frac{d\hat{\kappa}_d}{\varepsilon_f}\right)\bar{\boldsymbol{\sigma}} \tag{A1}$$

The effective stress increment is given by:

$$d\bar{\boldsymbol{\sigma}} = \mathbf{D_e} : (d\boldsymbol{\varepsilon} - d\boldsymbol{\varepsilon}_p) = \mathbf{D}_e : d\boldsymbol{\varepsilon} - \Delta\lambda\mathbf{D}_e : \left(\frac{\partial \mathbf{m}_p}{\partial\bar{\boldsymbol{\sigma}}} : d\bar{\boldsymbol{\sigma}} + \frac{\partial \mathbf{m}_p}{\partial\kappa_p}d\kappa_p\right) - d\lambda\mathbf{D}_e : \mathbf{m}_p \tag{A2}$$

where plastic strain $\boldsymbol{\varepsilon}_p = \Delta\lambda\mathbf{m}_p$ and $\mathbf{m}_p = \frac{\partial g_p}{\partial\boldsymbol{\sigma}}$ is the plastic flow direction.

With some rearrangements, the following form is obtained:

$$d\bar{\boldsymbol{\sigma}} = \mathbf{D}_a : d\boldsymbol{\varepsilon} - \mathbf{D}_a : \left(\Delta\lambda\frac{\partial \mathbf{m}_p}{\partial\kappa_p}k_p + \mathbf{m}_p\right)d\lambda \tag{A3}$$

where $\mathbf{D}_a = \left[\mathbf{D}_e^{-1} + \Delta\lambda\frac{\partial \mathbf{m}_p}{\partial\boldsymbol{\sigma}}\right]^{-1}$ and $\dot{\kappa}_p = k_p\dot{\lambda}$ as defined in Eq. (6).

From the consistent linearization of the yield equation, we have:

$$df_p = \frac{\partial f_p}{\partial\bar{\boldsymbol{\sigma}}} : d\bar{\boldsymbol{\sigma}} + \frac{\partial f_p}{\partial q_h}\frac{\partial q_h}{\partial\kappa_p}d\kappa_p = 0 \Rightarrow \frac{\partial f_p}{\partial\bar{\boldsymbol{\sigma}}} : d\bar{\boldsymbol{\sigma}} = H_a d\lambda \tag{A4}$$

where $H_a = -\frac{\partial f_p}{\partial q_h}\frac{\partial q_h}{\partial\kappa_p}k_p$

Substitute Eq. (A3) into (A4) to express $d\lambda$ in terms of $d\boldsymbol{\varepsilon}$:

$$d\lambda = \left(\frac{\frac{\partial f_p}{\partial\bar{\boldsymbol{\sigma}}} : \mathbf{D}_a}{H_a + \frac{\partial f_p}{\partial\bar{\boldsymbol{\sigma}}} : \mathbf{D}_a : \left(\Delta\lambda\frac{\partial \mathbf{m}}{\partial\kappa_p}k_p + \mathbf{m}_p\right)}\right) : d\boldsymbol{\varepsilon} \tag{A5}$$

From Eq. (A5), the effective stress increment (A3) can now be expressed in terms of $d\boldsymbol{\varepsilon}$:

$$d\bar{\boldsymbol{\sigma}} = \mathbf{D}_{ep}^{al} : d\boldsymbol{\varepsilon}$$

$$\mathbf{D}_{ep}^{al} = \mathbf{D}_a - \frac{\mathbf{D}_a : \left(\Delta\lambda\frac{\partial \mathbf{m}_p}{\partial\kappa_p}k_p + \mathbf{m}_p\right) \otimes \frac{\partial f_p}{\partial\bar{\boldsymbol{\sigma}}} : \mathbf{D}_a}{H_a + \frac{\partial f_p}{\partial\bar{\boldsymbol{\sigma}}} : \mathbf{D}_a : \left(\Delta\lambda\frac{\partial \mathbf{m}_p}{\partial\kappa_p}k_p + \mathbf{m}_p\right)} \tag{A6}$$

We can now derive the expression for $d\kappa_d$:

$$\Delta\kappa_d = \frac{\Delta\lambda\mathbf{m}_v}{x_s}$$

$$d\kappa_d = d\lambda\frac{\mathbf{m}_v}{x_s} + \frac{\Delta\lambda}{x_s}\left(\frac{\partial \mathbf{m}_v}{\partial\bar{\boldsymbol{\sigma}}} : d\bar{\boldsymbol{\sigma}} + \frac{\partial \mathbf{m}_v}{\partial\kappa_p}d\kappa_p\right) - \frac{\Delta\lambda}{x_s^2}\frac{\partial x_s}{\partial\bar{\boldsymbol{\sigma}}} : d\bar{\boldsymbol{\sigma}} \tag{A7}$$

Finally, we substitute Eqs. (A5) and (A6a) into (A7b) to obtain $d\kappa_d$ in terms of $d\boldsymbol{\varepsilon}$:

$$d\kappa_d = \mathbf{N}_a : d\boldsymbol{\varepsilon} \tag{A8}$$

where

$$\mathbf{N}_a = \left\{\frac{m_v}{x_s}\left[\frac{\frac{\partial f_p}{\partial\bar{\boldsymbol{\sigma}}} : \mathbf{D}_a}{H_a + \frac{\partial f_p}{\partial\bar{\boldsymbol{\sigma}}} : \mathbf{D}_a : \left(\Delta\lambda\frac{\partial \mathbf{m}_p}{\partial\kappa_p}k_p + \mathbf{m}_p\right)}\right] + \left[\frac{\Delta\lambda}{x_s}\left(\frac{\partial m_v}{\partial\bar{\sigma}_v}\frac{\boldsymbol{\delta}}{3} + \frac{\partial m_v}{\partial\bar{\rho}}\frac{\bar{\mathbf{s}}}{\bar{\rho}}\right) - \frac{\Delta\lambda m_v}{x_s^2}\frac{\partial x_s}{\partial\boldsymbol{\sigma}}\right] : \mathbf{D}_{ep}^{al}\right\}$$

The nominal stress increment $d\boldsymbol{\sigma}$ in Eq. (A1) can now be expressed in terms of $d\boldsymbol{\varepsilon}$ and $d\bar{\kappa}_d$:

$$d\boldsymbol{\sigma} = (1-\omega)\mathbf{D}_{ep}^{al} : d\boldsymbol{\varepsilon} - \exp\left(\frac{-\hat{\kappa}_d}{\varepsilon_f}\right)\left(\frac{1}{\varepsilon_f}\right)[m(d\bar{\kappa}_d) + (1-m)d\kappa_d]\bar{\boldsymbol{\sigma}}$$
$$= \left[(1-\omega)\mathbf{D}_{ep}^{al} - \exp\left(\frac{-\hat{\kappa}_d}{\varepsilon_f}\right)\left(\frac{1}{\varepsilon_f}\right)(1-m)\bar{\boldsymbol{\sigma}} \otimes \mathbf{N}_a\right] : d\boldsymbol{\varepsilon}$$
$$- \left[\exp\left(\frac{-\hat{\kappa}_d}{\varepsilon_f}\right)\left(\frac{m}{\varepsilon_f}\right)\bar{\boldsymbol{\sigma}}\right]d\bar{\kappa}_d \quad \text{(A9)}$$

References

ABAQUS, 2003. Standard User's Manual Version 6.4. Hibbit, Karlsson and Sorensen Inc.

Abu Al-Rub, R.K., Voyiadjis, G.Z., 2005. A direct finite element implementation of the gradient-dependent theory. International Journal for Numerical Methods in Engineering 63, 603–629.

Abu Al-Rub, R.K., Voyiadjis, G.Z., 2009. Gradient-enhanced coupled plasticity-anisotropic damage model for concrete fracture: computational aspects and applications. International Journal of Damage Mechanics 18, 115–154.

Addessi, D., Marfia, S., Sacco, E., 2002. A plastic nonlocal damage model. Computer Methods in Applied Mechanics and Engineering 191, 1291–1310.

Bažant, Z.P., 1976. Instability, ductility, and size effects in strain-softening concrete. ASCE Journal of Engineering Mechanics Division 102, 331–344.

Bažant, Z.P., Belytschoko, T., Chang, T.P., 1984. Continuum model for strain softening. Journal of Structural Engineering 110, 1666–1692.

Bažant, Z.P., Jirásek, M., 2003. Nonlocal integral formulations of plasticity and damage: survey of progress. Journal of Engineering Mechanics, 21–51.

Bažant, Z.P., Oh, B.H., 1983. Crack band theory for fracture of concrete. Materiaux et Constructions, Materials and Structures 16, 155–177.

Bažant, Z.P., Pijaudier-Cabot, G., 1989. Measurement of characteristic length of nonlocal continuum. Journal of Engineering Mechanics 115, 755–767.

Belnoue, J.P., Nguyen, G.D., Korsunsky, A.M., 2007. A one-dimensional nonlocal damage-plasticity model for ductile materials. International Journal of Fracture 144, 53–60.

Chaboche, J.L., Lesne, P.M., Maire, J.F., 1995. Continuum damage mechanics, anisotropy and damage deactivation for brittle materials like concrete and ceramic composites. International Journal of Damage Mechanics 4, 5–22.

Cicekli, U., Voyiadjis, G.Z., Abu Al-Rub, R.K., 2007. A plasticity and anisotropic damage model for plain concrete. International Journal of Plasticity 23, 1874–1900.

de Borst, R., Pamin, J., 1996. Some novel developments in finite element procedures for gradient-dependent plasticity. International Journal for Numerical Methods in Engineering 39, 2477–2505.

de Borst, R., Pamin, J., Geers, M.G.D., 1999. On coupled gradient-dependent plasticity and damage theories with a view to localization analysis. European Journal of Mechanics, A/Solids 18, 939–962.

Di Luzio, G., 2007. A symmetric over-nonlocal microplane model M4 for fracture in concrete. International Journal of Solids and Structures 44, 4418–4441.

Di Luzio, G., Bažant, Z.P., 2005. Spectral analysis of localization in nonlocal and over-nonlocal materials with softening plasticity or damage. International Journal of Solids and Structures 42, 6071–6100.

Forest, S., 2009. Micromorphic approach for gradient elasticity, viscoplasticity, and damage. Journal of Engineering Mechanics 135, 117–131.

Gatuingt, F., Pijaudier-Cabot, G., 2002. Coupled damage and plasticity modelling in transient dynamic analysis of concrete. International Journal for Numerical and Analytical Methods in Geomechanics 26, 1–24.

Geers, M.G.D., de Borst, R., Peerlings, R.H.J., 2000. Damage and crack modeling in single-edge and double-edge notched concrete beams. Engineering Fracture Mechanics 65, 247–261.

Gopalaratnam, V.S., Shah, S.P., 1985. Softening response of plain concrete in direct tension. Journal of the American Concrete Institute 82, 310–323.

Grassl, P., Jirásek, M., 2006a. Damage-plastic model for concrete failure. International Journal of Solids and Structures 43, 7166–7196.

Grassl, P., Jirásek, M., 2006b. Plastic model with non-local damage applied to concrete. International Journal for Numerical and Analytical Methods in Geomechanics 30, 71–90.

Jirásek, M., Grassl, P., 2004. Nonlocal plastic models for cohesive-frictional materials. In: Vermeer, P.A., Vermeer, W., Ehlers, H.J. (Eds.), Continuous and Discontinuous Modeling of Cohesive-Frictional Materials. A.A. Balkema Publishers, Leiden, The Netherlands, pp. 323–337.

Jirásek, M., Grassl, P., 2008. Evaluation of directional mesh bias in concrete fracture simulations using continuum damage models. Engineering Fracture Mechanics 75, 1921–1943.

Kupfer, H., Hilsdorf, H.K., Rusch, H., 1969. Behavior of concrete under biaxial stresses. Journal of the American Concrete Institute 66, 656–666.

Mohamad-Hussein, A., Shao, J.F., 2007. Modelling of elastoplastic behaviour with non-local damage in concrete under compression. Computers & Structures 85, 1757–1768.

Nguyen, G.D., Korsunsky, A.M., 2008. Development of an approach to constitutive modelling of concrete: isotropic damage coupled with plasticity. International Journal of Solids and Structures 45, 5483–5501.

Peerlings, R.H.J., De Borst, R., Brekelmans, W.A.M., De Vree, J.H.P., 1996. Gradient enhanced damage for quasi-brittle materials. International Journal for Numerical Methods in Engineering 39, 3391–3403.

Peerlings, R.H.J., de Borst, R., Brekelmans, W.A.M., Geers, M.G.D., 1998. Gradient-enhanced damage modelling of concrete fracture. Mechanics of Cohesive-Frictional Materials 3, 323–342.

Peerlings, R.H.J., Geers, M.G.D., de Borst, R., Brekelmans, W.A.M., 2001. A critical comparison of nonlocal and gradient-enhanced softening continua. International Journal of Solids and Structures 38, 7723–7746.

Poh, L.H., Swaddiwudhipong, S., 2009. Gradient-enhanced softening material models. International Journal of Plasticity, doi.10.1016/j.ijplas.2009.1001.1003.

Samal, M.K., Seidenfuss, M., Roos, E., Dutta, B.K., Kushwaha, H.S., 2008. Finite element formulation of a new nonlocal damage model. Finite Elements in Analysis and Design 44, 358–371.

Schlangen, E., 1993. Experimental and numerical analysis of fracture processes in concrete. Dissertation. Delft University of Technology.

Stromberg, L., Ristinmaa, M., 1996. FE-formulation of a nonlocal plasticity theory. Computer Methods in Applied Mechanics and Engineering 136, 127–144.

Van Mier, J.G.M., Nooru-Mohamed, M.B., 1990. Geometrical and structural aspects of concrete fracture. Engineering Fracture Mechanics 35, 617–628.

Vermeer, P.A., Brinkgreve, R.B.J., 1994. A new effective non-local strain measure for softening plasticity. In: Chambon, R., Desrues, J., Vardoulakis, I., (Eds.), Localisation and Bifurcation Theory for Soils and Rocks. Balkema, pp. 89–100.

Voyiadjis, G.Z., Taqieddin, Z.N., Kattan, P.I., 2008. Anisotropic damage-plasticity model for concrete. International Journal of Plasticity 24, 1946–1965.

Wu, J.Y., Li, J., Faria, R., 2006. An energy release rate-based plastic-damage model for concrete. International Journal of Solids and Structures 43, 583–612.